1-1-2010

Tricarbonylrhenium(I) and Manganese(I) Complexes of 2-(pyrazolyl)-4-toluidine

Brendan J Liddle
Marquette University

Sarath Wanniarachchi
Marquette University, sarath.wanniarachchi@marquette.edu

Sergey V. Lindeman
Marquette University, sergey.lindeman@marquette.edu

James R. Gardinier
Marquette University, james.gardinier@marquette.edu

Journal of Organometallic Chemistry, Vol. 695, No. 1 (January 2010): 53-61. DOI.

Tricarbonylrhenium(I) And Manganese(I) Complexes Of 2-(Pyrazolyl)-4-Toluidine

Brendan J. Liddle
Department of Chemistry, Marquette University, Milwaukee, WI
Sarath Wanniarachchi
Department of Chemistry, Marquette University, Milwaukee, WI
Sergey V. Lindeman
Department of Chemistry, Marquette University, Milwaukee, WI
James R. Gardinier
Department of Chemistry, Marquette University, Milwaukee, WI

Abstract

A series of tricarbonyl rhenium(I) and manganese(I) complexes of the electroactive 2-(pyrazolyl)-4-toluidine ligand, H(pzAn^{Me}), has been prepared and characterized including by single crystal X-ray diffraction studies. The reactions between H(pzAn^{Me}) and M(CO)$_5$Br afford *fac*-MBr(CO)$_3$[H(pzAn^{Me})] (M = Mn, **1a**; Re, **1b**) complexes. The ionic species {*fac*-M(CH$_3$CN)(CO)$_3$[H(pzAn^{Me})]}(PF$_6$) (M = Mn, **2a**; Re, **2b**) were prepared by metathesis of **1a** or **1b** with TlPF$_6$ in acetonitrile. Complexes **1a** and **1b** partly

ionize to {M(CH_3CN)$(CO)_3$[H($pzAn^{Me}$)]$^+$}(Br^-) in CH_3CN but retain their integrity in less donating solvents such as acetone or CH_2Cl_2. Each of the four metal complexes reacts with (NEt_4)(OH) in CH_3CN to give poorly-soluble crystalline [*fac*-M$(CO)_3$(μ-$pzAn^{Me}$)]$_2$ (M = Mn, **3a**; Re, **3b**). The solid state structures of **3a** and **3b** are of centrosymmetric dimeric species with bridging amido nitrogens and with pyrazolyls disposed *trans*- to the central planar M_2N_2 metallacycle. In stark contrast to the diphenylboryl derivatives, $Ph_2B(pzAn^{Me})$, none of the tricarbonyl group 7 metal complexes are luminescent.

Graphical abstract

Tricarbonyl group 7 metal complexes of the electroactive N,N-chelating 2-(pyrazolyl)-4-toluidine ligand, H($pzAn^{Me}$), have been prepared and characterized in solution and in the solid state in an effort to ascertain whether switching behavior could be mediated by Brønsted acids and bases. The electronic properties and periodic trends are discussed.

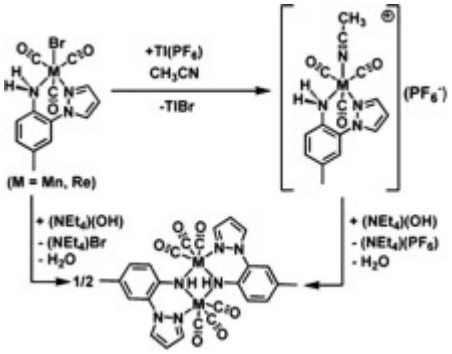

Keywords

Group 7 metal tricarbonyls, Group 7 amidos, IR spectroscopy, NMR spectroscopy, Electrochemistry

1. Introduction

There has been continued interest in $Re^I(CO)_3$ chelate complexes owing to their potential biomedical applications [1] as well as to the promising photophysical behavior derived from MLCT transitions [2] that can be exploited in energy and electron transfer studies [3], in display technology [4], and even in solar energy conversion and photocatalysis [5]. We have been exploring the reactivity and properties of luminescent complexes of electroactive N,N-chelating ligands based on 2-(pyrazolyl)-4-toluidine, H($pzAn^{Me}$), and other allied derivatives for the latter purposes [6], [7], [8]. For instance, our early studies indicated that the simple Lewis adduct of H($pzAn^{Me}$) and BPh_3 is a thermally unstable species with distinct cyan emission that gives way to the intensely green-blue fluorescent $Ph_2B(pzAn^{Me})$ via elimination of benzene [6]. In this latter case, DFT calculations and experimental observations indicated that emission was a result of a π–π* transition involving the chelated ($pzAn^{Me}$)$^-$ portion of the complex. Unfortunately, this complex is readily susceptible to solvolysis by alcohols or other protic media. Changing the electronic properties of the ligands by substitution at the 2- or 4- position of the aniline moiety permits a good control over tuning the emission properties (ranging from blue to yellow-green) and can greatly improve stability of the resulting dyes toward solvolysis [6], [7]. We became interested exploring the transition metal chemistry of this ligand scaffold [8] with the hope of discovering complexes that are more robust or kinetically inert and that might possess more unusual electronic properties or even more desirable chemical reactivities than

the diphenylboron derivatives. An added incentive to this area of study is that the electronic properties of the transition metal complexes might be chemically switchable by addition of Brønsted acids or bases as in Scheme 1. That is, the capacity for the metal-coordinated aniline ligand to become involved in ligand-centered one-electron oxidation or possibly even metal-nitrogen multiple bonding should be greatly impaired when the aniline nitrogen is coordinatively-saturated, as in the left of Scheme 1. Also, the extent to which the ligand pi-system is conjugated becomes attenuated upon quarternization of nitrogen such that significant changes in the optoelectronic properties of the resultant complexes would be anticipated. We were aware of recent sporadic reports concerning various nickel and palladium complexes of H(pz*An) (pz* = 3,5-dimethylpyrazolyl; An = aniline) and related derivatives [9], [10] but surprisingly few details concerning the electronic properties of these transition metal complexes were disseminated. Given the enticing photophysical prospects of tricarbonylrhenium(I) N,N-chelates we detail our initial findings concerning the preparation, reactivity, and electronic properties of the H(pzAn^{Me}) complexes of this moiety. We also document our findings concerning the manganese(I) congeners with the intent of providing insight into changes in electronic properties and reactivity as a function of the periodicity of the group 7 metals.

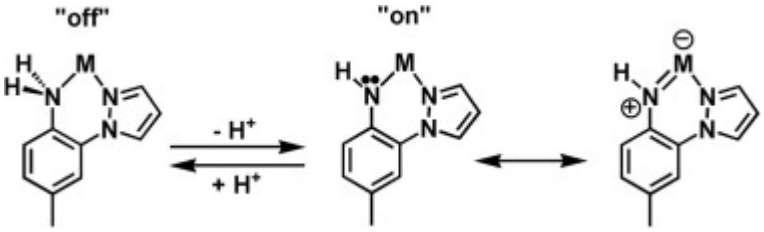

Scheme 1.

2. Experimental

2.1. Materials

The compounds $Mn(CO)_5Br$, $TlPF_6$, NEt_4OH were purchased from commercial sources and were used without further purification while $Re(CO)_5Br$ [11] and H(pzAn^{Me}) [6] were prepared by literature methods. The solvents used in the preparations were dried by conventional methods and distilled under nitrogen prior to use. All reactions were performed under an atmosphere of nitrogen using Schlenk techniques.

2.2. Physical measurements

Midwest MicroLab, LLC, Indianapolis, Indiana 45250, performed all elemental analyses. ^1H, ^{13}C, ^{19}F and ^{31}P NMR spectra were recorded on a Varian 400 MHz spectrometer. Chemical shifts were referenced to solvent resonances at δ_H 7.27, δ_C 77.23 for $CDCl_3$; δ_H 5.33 for CD_2Cl_2; δ_H 1.94, δ_C 118.9 for CD_3CN and δ_H 2.05, δ_C 29.92 for acetone-d_6 while those for ^{19}F and ^{31}P NMR spectra were referenced against external standards of $CFCl_3$ (δ_F 0.00 ppm) and 85% $H_3PO_{4(aq)}$ (δ_P 0.00 ppm), respectively. Melting point determinations were made on samples contained in glass capillaries using an Electrothermal 9100 apparatus and are uncorrected. Absorption measurements were recorded on an Agilent 8453 spectrometer. Electrochemical measurements were collected under nitrogen atmosphere at a scan rate of 50 mV/s for samples as 0.1 mM CH_3CN solutions with 0.1 M NBu_4PF_6 as the supporting electrolyte. A three-electrode cell comprised of an Ag/AgCl electrode (separated from the reaction

medium with a semipermeable polymer membrane filter), a platinum working electrode, and a glassy carbon counter electrode was used for the voltammetric measurements. With this set up, the ferrocene/ferrocenium couple had an $E_{1/2}$ value of +0.53 V consistent with the literature value in this solvent [12].

2.3. Synthesis of complexes

2.3.1. Synthesis of *fac*-$MnBr(CO)_3[H(pzAn^{Me})]$ (**1a**)

A mixture of 0.495 g (1.80 mmol) $Mn(CO)_5Br$ and 0.312 g (1.80 mmol) $H(pzAn^{Me})$ in 25 ml of toluene was heated at reflux 4 h initially giving an orange solution, then a yellow precipitate. After cooling, the yellow precipitate was isolated by filtration, washed with three 10 ml portions Et_2O, and then dried under vacuum to give 0.579 g (82%) of pure **1a** as a yellow powder. M.p.: 215–223 °C, dec. Anal. Calc. for $C_{13}H_{11}BrMnN_3O_3$: C, 39.82; H, 2.83; N, 10.72. Found: C, 39.56; H, 3.07; N, 10.44%. IR (KBr, cm^{-1}) ν_{co} 2029, 1923, 1902; (CH_2Cl_2, cm^{-1}) ν_{co} 2033, 1940, 1919; (CH_3CN, cm^{-1}) ν_{co} major: 2029, 1936, 1913; minor: 2050, 1954. ^1H NMR (CD_2Cl_2): δ_H 8.31 (s, 1H, H_3-pz), 8.12 (s, 1H, H_5-pz), 7.29 (s, 1H, H_3-An), 7.22 (br s, 2H, $H_{5/6}$-An), 6.72 (s, 1 H, H_4-pz), 4.98 (br s, 1H, NH_a), 4.10 (br s, 1H, NH_b), 2.43 (s, 3H, CH_3). ^1H NMR (CD_3CN): (major resonances only, see Supporting information) δ 8.23 (br s, 2H, $H_{3\&5}$-pz), 7.40–7.20 (br m, 3H, H_3,H_5,H_6-An), 6.71 (s, 1H, H_4-pz), 5.85 (br s., 1H, NH), 4.09 (br s, 1H, NH), 2.38 (s, 3H, CH_3). ^{13}C NMR (CD_3CN): δ_C 140.9, 136.9, 135.2, 133.3, 132.0, 129.6, 123.6, 121.4, 109.8, 20.6. UV–Vis (CH_3CN) λ_{max}, nm (ε, M^{-1} cm^{-1}): 213 (43,200), 256 (16 900), 284 (10 100), 371 (1600). E1/2ox (V vs. Ag/AgCl: ΔE (E_a − E_c, mV): i_c/i_a): 0.98 V: 120 mV: 0.44. Single crystals of **1a** suitable for X-ray diffraction studies were grown by layering a dichloromethane solution with hexanes and allowing solvents to diffuse.

2.3.2. Synthesis of *fac*-$ReBr(CO)_3[H(pzAn^{Me})]$ (**1b**)

A mixture of 0.526 g (1.30 mmol) $Re(CO)_5Br$ and 0.225 g (1.30 mmol) $H(pzAn^{Me})$ in 20 ml of toluene was heated at reflux 4 h giving a colorless precipitate. After cooling to room temperature, the precipitate was isolated by filtration, washed with two 5 mL portions Et_2O, and then dried under vacuum 12 h to give 0.582 g (86%) of **1b** as a colorless powder. M.p.: 294–306 °C, dec. to black solid. Anal. Calc. for $C_{13}H_{11}BrN_3O_3Re$: C, 29.83; H, 2.12; N, 8.03. Found: C, 29.65; H, 2.24; N, 8.37%. IR (KBr, cm^{-1}) ν_{co} 2019, 1903, 1884; (CH_2Cl_2, cm^{-1}) ν_{co} 2029, 1921, 1900; (CH_3CN, cm^{-1}) ν_{co} major: 2025, 1917, 1894; minor: 2040, 1935. ^1H NMR (CD_2Cl_2): δ_H 8.16 (dd, J = 2, 1 Hz, 1H, H_3-pz), 8.09 (dd, J = 3, 1 Hz, 1H, H_5-pz), 7.31 (s, 1H, H_3-An), 7.28 (part of AB m, 1H, H_5/$_6$-An), 7.19 (part of AB m, 1H, $H_{5/6}$-An), 6.73 (dd, J = 3, 2 Hz, 1H, H_4-pz), 5.29 (br d, J = 11 Hz, 1H, NH_a), 4.60 (br d, J = 11 Hz, 1H, NH_b), 2.46 (s, 3H, CH_3). ^1H NMR (CD_3CN): δ_H 8.27 (dd, J = 3, 1 Hz, 1H, H_5-pz), 8.10 (dd, J = 2, 1 Hz, 1H, H_3-pz), 7.42 (s, 1H, H_3-An), 7.25 (AB m, 2H, H_5- and H_6-An), 6.72 (dd, J = 3, 2 Hz, 1 H, H_4-pz), 6.29 (br d, J = 12 Hz, 1H, NH_a), 4.73 (br d, J = 12 Hz, 1H, NH_b), 2.40 (s, 3H, CH_3). ^{13}C NMR (CD_3CN): δ_C 210, 207, 149, 138, 135, 133, 132, 130, 125, 122, 110, 21. UV–Vis (CH_3CN) λ_{max}, nm (ε, M^{-1} cm^{-1}): 219 (16 600), 249 (8100), 286 (2800), 303 (1200). E1/2ox ((E_a + E_c)/2 V, ΔE (E_a − E_c) mV, i_c/i_a): 1.32 V, 120 mV, 0.55. Single crystals of **1b** suitable for X-ray diffraction studies were grown by layering a dichloromethane solution with hexanes and allowing solvents to diffuse.

2.3.3. Synthesis of {*fac*-$Mn(CH_3CN)(CO)_3[H(pzAn^{Me})]$}($PF_6$) (**2a**)

A mixture of 0.393 g (1.00 mmol) **1a** and 0.350 g (1.00 mmol) $TlPF_6$ in 20 mL dry acetonitrile was heated at reflux for 20 h under nitrogen. After cooling to room temperature, the yellow solution

of **2a** and colorless precipitate (TlBr) were separated by cannula filtration. Solvent was removed under vacuum to leave 0.442 g (89%) of **2a** as a yellow powder. M.p.: 192–196 °C dec. Anal. Calc. for $C_{15}H_{14}F_6MnN_4O_3P$: C, 36.16; H, 2.83; N, 11.25. Found: C, 36.12; H, 2.97; N, 11.43%. IR (KBr, cm^{-1}) ν_{co} 2052, 1956, 1919; (CH_2Cl_2, cm^{-1}) ν_{co} 2052, 1954; (CH_3CN, cm^{-1}) ν_{co} 2050, 1954. ^1H NMR (CD_2Cl_2): δ_H 8.20 (s, 1H, H_5-pz), 8.05 (s, 1H, H_3-pz), 7.30 (br part of AB, 1H, Ar), 7.29 (s, 1H, Ar), 7.25 (br part of AB, 1H, Ar), 6.79 (br s, 1H, H_4-pz), 5.01 (br d, J = 11.6 Hz, 1H, NH), 4.17 (br d, J = 11.6 Hz, 1H, NH), 2.44 (s, 3H, $ArCH_3$), 2.32 (s, 3H, CH_3CN). ^1H NMR (CD_3CN): δ_H 8.31 (s, 1H, H_5-pz), 8.14 (s, 1H, H_3-pz), 7.39 (s, 1H, Ar), 7.31 (br part of AB, 1H, Ar), 7.21 (br part of AB, 1H, Ar), 6.76 (br s, 1H, H_4-pz), 5.57 (br s, 1H, NH), 4.60 (br s, 1H, NH), 2.35 (br s, 3H, $ArCH_3$), 1.96 (br s, 8H, CH_3CN and residual solvent of CD_3CN). ^{13}C NMR (CD_3CN): resonances not resolved. ^{19}F NMR (CD_3CN): δ_F −72.7 (J_{FP} = 707 Hz). ^{31}P NMR (CD_3CN): δ_P −144.6 (J_{PF} = 707 Hz). UV–Vis (CH_3CN) λ_{max}, nm (ε, M^{-1} cm^{-1}): 213 (37 100), 255 (14 800), 281 (9200), 371 (1600). E1/2ox ((E_a + E_c)/2 V, ΔE (E_a − E_c) mV, i_c/i_a): 1.42 V, 150 mV, 0.33. Single crystals of **2a** suitable for X-ray diffraction studies were grown by layering a dichloromethane solution with Et_2O and allowing the solvents to slowly diffuse.

2.3.4. Synthesis of {*fac*-Re(CH_3CN)$(CO)_3$[H($pzAn^{Me}$)]}(PF_6) (**2b**)

A mixture of 0.136 g (0.259 mmol) **1b** and 0.090 g (0.26 mmol) $TlPF_6$ in 20 mL dry acetonitrile was heated at reflux for 20 h under nitrogen. After cooling to room temperature, the colorless solution of **2b** and precipitate (TlBr) were separated by cannula filtration. Solvent was removed under vacuum to leave 0.163 g (78%) of **2b** as a colorless powder. M.p.: 165–186 °C dec. to black solid. Anal. Calc. for $C_{15}H_{14}F_6N_4O_3PRe$: C, 28.62; H, 2.24; N, 8.90. Found: C, 28.55; H, 2.02; N, 8.99%. IR: (KBr, cm^{-1}) ν_{co} 2035, 1925, 1905; (CH_2Cl_2, cm^{-1}) ν_{co} 2044, 1936; (CH_3CN, cm^{-1}) ν_{co} 2040, 1935. ^1H NMR (CD_2Cl_2): δ_H 8.19 (dd, J = 2, 1 Hz, 1H, H_5-pz), 8.05 (dd, J = 3, 1 Hz, 1H, H_3-pz), 7.31 (br part of AB, 1H, Ar), 7.30 (s, 1H, Ar), 7.26 (br part of AB, 1H, Ar), 6.80 (dd, J = 3, 2 Hz, 1H, H_4-pz), 5.32 (br d, J = 12 Hz, 1H, NH), 5.14 (br d, J = 12 Hz, 1H, NH), 2.46 (s, 3H, $ArCH_3$), 2.41 (s, 3H, CH_3CN). ^1H NMR (CD_3CN): δ_H 8.34 (d, J = 3 Hz, 1H, H_5-pz), 8.14 (d, J = 2 Hz, 1H, H_3-pz), 7.45 (s, 1H, H_3-An), 7.32 (AB m, 2H, H_5- and H_6-An), 6.79 (dd, J = 3, 2 Hz, 1 H, H_4-pz), 6.36 (br d, J = 12 Hz, 1H, NH_a), 5.83 (br d, J = 12 Hz, 1H, NH_b), 2.41 (s, 3H, CH_3-An), 2.22 (s, 3H, CH_3CN-Re). ^{13}C NMR (CD_3CN): δ_C 193.4, 192.2, 148.7, 138.8, 133.9, 132.3, 130.8, 125.4, 123.7, 122.9, 118.5, 110.9, 20.7, 3.99. UV–Vis (CH_3CN) λ_{max}, nm (ε, M^{-1} cm^{-1}): 216 (18 000), 251 (7600), 285 (3800), 307 (1200). ^{19}F NMR (CD_3CN): δ_F −72.9 (J_{FP} = 707 Hz). ^{31}P NMR (CD_3CN): δ_P −144.6 (J_{PF} = 707 Hz). E1/2ox ((E_a + E_c)/2 V, ΔE (E_a − E_c) mV, i_c/i_a): 1.76 V, 110 mV, 0.34. Single crystals of **2b** suitable for X-ray diffraction studies were grown by vapor diffusion of Et_2O into a CH_2Cl_2 solution of the complex.

2.3.5. Synthesis of [*fac*-Mn$(CO)_3$(μ-$pzAn^{Me}$)]$_2$ (**3a**)

A 2.6 mL aliquot of a 0.10 M solution (0.26 mmol) of (NEt_4)(OH) in MeOH was added to a solution of 0.100 g (0.255 mmol) **1a** in 4 mL MeCN which immediately gave a yellow-brown solution. After leaving the solution undisturbed and protected from light for 5 d, the very dark solution was decanted from the yellow crystals and a thin layer of manganese metal (on the walls of the reaction vessel). The crystals were mechanically separated, washed with Et_2O, and dried under vacuum to give 0.016 g (20%) of **3a**. M.p.: 265–282 °C. Anal. Calc. for $C_{26}H_{20}Mn_2N_6O_6$: C, 50.18; H, 3.24; N, 13.50. Found: C, 50.12; H, 2.97; N, 13.13%. IR (KBr, cm^{-1}) ν_{co} 2002, 1905, 1884; (CH_3CN, cm^{-1}) ν_{co} 2004, 1906. ^1H NMR (CD_3CN): δ_H 8.62 (d, J = 2 Hz, 1H, H_5-pz), 8.50 (d, J = 1 Hz, 1H, H_3-pz), 7.45 (s, 1H), 7.09 (part of AB, 1H), 7.01 (dd, J = 2,1 Hz, 1H, H_4-pz), 6.97 (part of AB, 1H), 2.35 (s, 3H); NH not observed. ^{13}C NMR (CD_3CN):

not sufficiently soluble for reasonable acquisition times. UV–Vis (CH_3CN) λ_{max}, nm (absorbance of saturated solution): 235 (2.101), 286 (0.630), 326 (0.322), 368 (0.174). X-ray quality crystals removed directly from the mother liquor (without washing and drying) were found to contain two acetonitrile molecules of solvation per formula unit, **3a·2CH₃CN**.

2.3.6. Synthesis of [*fac*-$Re(CO)_3(\mu\text{-}pzAn^{Me})]_2$ (**3b**)

2.3.6.1. Method A (from 1b)

A 2.3 mL portion of 0.10 M (0.23 mmol) solution of $(NEt_4)(OH)$ in MeOH was added to a solution of 0.120 g (0.229 mmol) **1b** in 20 mL CH_3CN, which immediately gave a yellow solution. The yellow color dissipated within minutes and over several hours colorless blocks began to form. After two days left undisturbed, the crystals were isolated by filtration and drying under vacuum to give 0.052 g (51%) of **3b**. M.p.: 278–290 °C dec. to black solid. Anal. Calc. for $C_{26}H_{20}N_6O_6Re_2$: C, 35.29; H, 2.28; N, 9.50. Found: C, 35.65; H, 2.00; N, 9.17%. IR: (KBr, cm^{-1}) ν_{co} 2006, 1886, 1873; (CH_3CN, cm^{-1}) ν_{co} 2007, 1893. ^1H NMR (CD_3CN): δ_H 8.60 (d, J = 2 Hz, 2H, H_5-pz), 8.37 (d, J = 1 Hz, 1H, H_3-pz), 7.45 (s, 1H, Ar), 7.06 (part of AB, 1H), 6.97 (dd, J = 2, 1 Hz, 1H, H_4-pz), 6.96 (part of AB, 1H), 3.48 (br s, 1H, NH), 2.39 (s, 3H, CH_3). δ_H (acetone-d_6): 8.85 (d, J = 2 Hz, 1H, H_5-pz), 8.61 (d, J = 1 Hz, 1H, H_3-pz), 7.57 (s, 1H, Ar), 7.15 (part of AB, 1H), 7.06 (dd, J = 2,1 Hz, 1H, H_4-pz), 7.03 (part of AB, 1H), 3.57 (br s, 1H, NH), 2.36 (s, 3H, CH_3). ^{13}C NMR (CD_3CN): not sufficiently soluble to obtain spectra in reasonable acquisition times. UV–Vis (CH_3CN) λ_{max}, nm (absorbance, saturated solution): 232 (0.737), 262 (0.393), 306 (0.119), 334 (0.042). X-ray quality crystals removed directly from the mother liquor (without drying) were found to contain two acetonitrile molecules of solvation per formula unit, **3b·2CH₃CN**.

2.3.6.2. Method B (from 2b)

A 1.62 mL portion of a 0.142 M (0.230 mmol) solution of $(NEt_4)(OH)$ in MeOH was added to a solution of 0.145 g (0.230 mmol) **2b** in 20 mL CH_3CN, which immediately gave a yellow solution. The yellow color dissipated within minutes and over several hours colorless blocks began to form. After two days left undisturbed, the crystals were isolated by filtration and drying under vacuum to give 0.048 g (47% yield) of **3b** whose spectroscopic characterization data were identical to above.

3. Computational details

Calculations utilized the Spartan'06 program suite [13], where gas phase structures of the metal complexes were optimized using the initial geometry (C_1 symmetry for **1a/b** and **2a/b** but C_i symmetry for **3a/b**) from X-ray structural studies as a starting point, then the BP86/6-31G* density functional theoretical model was employed owing to the demonstrated success of this model when applied to other complexes [14]. Analytical vibrational frequency calculations were also carried out on the computationally inexpensive **1a/b** and **2a/b** to verify that the optimized geometries were stationary points. In the current case, agreement between this model and the solid state structures was good with the computational model affording bond distances between 0.01 Å and 0.05 Å longer than experimental structures. Single point energy and time-dependent density functional calculations (for the first six singlet excited states for **1a/b** and **2a/b** but only the first two singlet excited states of **3a/b** owing to the demanding computational expense of the latter) were performed on the energy-minimized structures using the hybrid B3LYP method, which incorporates Becke's three-parameter exchange functional (B3) [15] with the Lee, Yang, and Parr (LYP) [16] correlation functional where the

LACVP* effective core potential [17] basis set was employed for each. Complete results are provided in the Supporting information.

4. Single crystal X-ray crystallography

X-ray intensity data from a yellow plate of **1a**, a colorless block of **1b**, a yellow block of **2a**, a colorless block of **2b**, a yellow prism of **3a·2CH$_3$CN**, and a colorless prism of **3b·2CH$_3$CN** were measured at 100(2) K (except **2b** which was collected at 130(2) K) with a Bruker AXS 3-circle diffractometer equipped with a Smart2 [18] CCD detector using either Cu Kα or Mo Kα radiation as indicated in Table 1, Table 2. Raw data frame integration and Lp corrections were performed with Saint+ [19]. Final unit cell parameters were determined by least-squares refinement of 5995 reflections from the data set of **1a**, 5750 reflections from the data set of **1b**, of 5222 reflections from that of **2a**, 6385 reflections from that of **2b**, 7062 reflections of **3a·2CH$_3$CN**, 5148 reflections from that of **3b·2CH$_3$CN**, 7188 reflections from that of **3·2CH$_3$CN**, with $I > 2\sigma(I)$ for each. Analysis of the data showed negligible crystal decay during collection in each case. Direct methods structure solutions, difference Fourier calculations and full-matrix least-squares refinements against F^2 were performed with Shelxtl [20]. Numerical absorption corrections based on the real shapes of the crystals were applied to the data of each **1a**, **2a**, and **3b·2CH$_3$CN** while semi-empirical absorption corrections based on the multiple measurement of equivalent reflections was applied to the data of each **1b**, **2b**, and **3a**·2**CH$_3$CN** with Sadabs [19]. All non-hydrogen atoms were refined with anisotropic displacement parameters. Hydrogen atoms were placed in geometrically idealized positions and included as riding atoms. The X-ray crystallographic parameters and further details of data collection and structure refinements are presented in Table 1, Table 2.

Table 1. Crystallographic data collection and structure refinement for **1a**, **2a**, and **3a·2CH$_3$CN**.

Compound	**1a**	**2a**	**3a·2CH$_3$CN**
Formula	$C_{13}H_{11}BrMnN_3O_3$	$C_{15}H_{14}F_6MnN_4O_3P$	$C_{30}H_{26}Mn_2N_8O_6$
Formula weight	392.10	498.21	704.47
Crystal system	Monoclinic	Triclinic	Triclinic
Space group	*P2$_1$/n*	P1$^-$	P1$^-$
a (Å)	10.9987(2)	12.5631(3)	7.8903(9)
b (Å)	11.5636(2)	10.9887(2)	8.6499(10)
c (Å)	11.5075(2)	21.2710(3)	11.7547(14)
α (°)	90	104.2360(10)	90.476(2)
β (°)	101.4420(10)	95.4760(10)	90.678(2)
γ (°)	90	101.0720(10)	102.619(2)
V (Å^3)	1434.49(4)	979.65(4)	782.78(16)
Z	4	2	1
T (K)	100(2)	100(2)	100(2)
ρ_{calc} (Mg m^{-3})	1.816	1.689	1.494
λ (Å)	1.54178	1.54178	0.71073
μ (mm^{-1})	10.877[a]	7.029[a]	0.863[b]
F(0 0 0)	776	500	360
ϑ Range (°)	5.08 to 67.02	3.79 to 61.12	1.73 to 31.89

Reflections collected	11 721	7913	12 823
Independent reflections [R_{int}]	2478 [0.0238]	2831 [0.0223]	4977 [0.0191]
Data/restraints/parameters	2478/0/234	2831/0/328	4977/0/260
Goodness of fit on F^2	1.004	0.989	0.973
$R[I > 2\sigma(I)]$[c](all data)	0.0232 (0.0254)	0.0330 (0.0383)	0.0291 (0.0331)
wR[d] (all data)	0.0550 (0.0559)	0.0864 (0.0873)	0.0761 (0.0785)
ρ_{fin} (max/min) (eÅ^{-3})	0.441/−0.261	0.440/−0.336	0.435/−0.196

[a]Cu Kα.

[b]Mo Kα.

[c] $R = \Sigma||F_o| - ||F_c||/\Sigma|F_o|$.

[d] $wR = [\sum w(|F_0^2| - |F_c^2|)^2/\sum w|F_0^2|^2]^{1/2}$.

Table 2. Crystallographic data collection and structure refinement for **1b**, **2b**, and **3b·2CH$_3$CN**.

Compound	**1b**	**2b**	**3b·2CH$_3$CN**
Formula	$C_{13}H_{11}BrReN_3O_3$	$C_{15}H_{14}F_6ReN_4O_3P$	$C_{30}H_{26}Re_2N_8O_6$
Formula weight	523.36	629.47	966.98
Crystal system	Monoclinic	Orthorhombic	Triclinic
Space group	*P2$_1$/n*	*Fdd2*	P1$^-$
a (Å)	11.0882(10)	17.3199(4)	7.8901(11)
b (Å)	11.6050(10)	24.0151(5)	8.7501(12)
c (Å)	11.5784(10)	19.0110(4)	11.8549(16)
α (°)	90	90	89.955(2)
β (°)	100.1730(10)	90	89.194(2)
γ (°)	90	90	77.629(2)
V (Å^3)	1466.5(2)	7907.4(3)	799.37(19)
Z	4	16	1
T (K)	100(2)	130(2)	100(2)
ρ_{calc} (Mg m^{-3})	2.370	2.115	2.009
λ (Å)	0.71073	1.54178	0.71073
μ (mm^{-1})	11.023[b]	13.563[a]	7.620[b]
F(0 0 0)	976	4800	460
θ Range (°)	2.34–31.82	5.94–61.41	2.38–31.88
Reflections collected	23 627	16 358	12 928
Independent reflections [R_{int}]	4737 [0.0462]	2973 [0.0209]	5068 [0.0242]
Data/restraints/parameters	4737/0/234	2973/1/281	5068/0/261
Goodness of fit on F^2	1.010	1.092	1.012
$R[I > 2\sigma(I)]$[c] (all data)	0.0245 (0.0283)	0.0167 (0.0171)	0.0150 (0.0161)
wR[d] (all data)	0.0601 (0.0617)	0.0414 (0.0416)	0.0353 (0.0356)
ρ_{fin} (max./min.) (e Å^{-3})	1.802/−1.831	0.418/−0.493	1.053/−1.002

aCu Kα.

bMo Kα.

c$R = \Sigma||F_o| - ||F_c||/\Sigma|F_o|$.
d $wR = [\sum w(|F_0^2| - |F_c^2|)^2/\sum w|F_0^2|^2]^{1/2}$.

5. Results and discussion

5.1. Syntheses

The ligand H(pzAn^{Me}) was prepared by exploiting modifications of Taillefer's [21] and Buchwald's [22] copper-catalyzed amination reaction between pyrazole and 2-bromo-4-toluidine which gives very good yield of desired product even on a 20 g scale, as described previously by our group [6]. The complexes MBr(CO)$_3$[H(pzAn^{Me})] (M = Mn (**1a**) or Re (**1b**)) were prepared in high yield by straightforward substitution reactions between M(CO)$_5$Br and H(pzAn^{Me}) in toluene (top of Scheme 2). The ionic species {M(CH$_3$CN)(CO)$_3$[H(pzAn^{Me})]}(PF$_6$) (M = Mn (**2a**) or Re (**2b**)), potentially useful starting materials for further reaction chemistry, are best prepared by metathesis of **1a** or **1b** with TlPF$_6$ in acetonitrile (middle of Scheme 2) to give the desired products in good yield [23]. The reactions between either **1a/b** or **2a/b** and one equivalent of (NEt$_4$)(OH) in CH$_3$CN (right of Scheme 2) afforded [M(CO)$_3$(μ-pzAn^{Me})]$_2$ (M = Mn (**3a**) or Re (**3b**)), in modest yields (ca. 30% for **3a** vs. about 50% for the rhenium derivative **3b**) as poorly-soluble crystalline solids after three days at room temperature. Analysis of the mother liquors of the product mixtures by ^{1}H NMR spectroscopy reveal the presence of free ligand H(pzAn^{Me}) and other unidentified products implicating hydrolysis and decomposition of resulting metal complexes as being responsible for the relatively low yields obtained from these reactions. Numerous synthetic routes and conditions (different bases, solvents, reaction temperatures) were explored to **3a/b** but the above preparative routes have most consistently afforded the highest yields of these complexes. The complexes **1a/b** and **2a/b** are slightly soluble in chlorinated solvents or THF, soluble in acetone, soluble with reaction (vide infra) in CH$_3$CN and more strongly donating solvents (DMF, DMSO, etc.) but are insoluble in hydrocarbons and Et$_2$O. Complexes **3a** and **3b** exhibit only very slight solubility in acetone or CH$_3$CN but are insoluble in most other organic solvents.

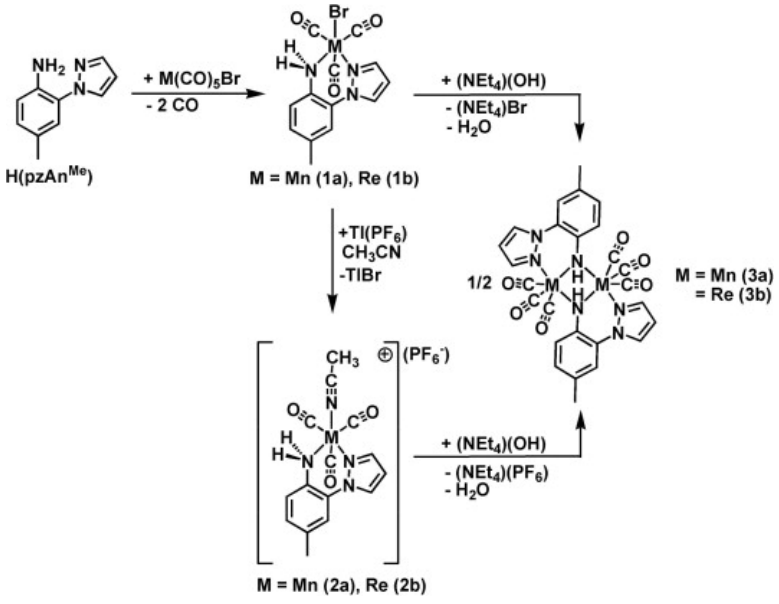

Scheme 2. Synthesis of group 7 tricarbonyl complexes of H(pzAn^{Me}).

5.2. Description of crystal structures

The solid state structures of all six new compounds **1a**, **1b**, **2a**, **2b**, **3a**·**2CH$_3$CN**, and **3b**·**2CH$_3$CN** were obtained from single-crystal X-ray diffraction experiments. The manganese and rhenium compounds are isostructural and the structures of the rhenium derivatives **1b**, **2b**, and **3b**·**2CH$_3$CN** are given in Fig. 1 while those of the manganese derivatives **1a**, **2a**, **3a**·**2CH$_3$CN** are included in the Supporting information. Selected bond distances and angles for all new compounds along are provided in Table 3. In all cases, the tricarbonylmetal(I) fragments are arranged in a *facial* manner as found for most other such complexes of N,N-chelating ligands. The compounds **1a/b** and **2a/b** are monomeric while **3a/b** are dimeric as a result of the amido group of the deprotonated aniline moiety bridging metal centers. For the dimeric species **3a** and **3b**, the molecules reside on inversion centers rendering each half of the dimer equivalent by symmetry. As anticipated from the relative sizes of the group 7 metals, the bond distances about the rhenium centers are typically 0.1 Å longer than those for the manganese complexes. The metal–nitrogen bonds involving the pyrazolyl portion of the ligand are detectably shorter than those involving the toluidinyl NH group (Table 3) and, for the manganese series (where all structural data were acquired at the same temperature, 100 K), the former bonds are longest for the starting bromide **1a** (Mn–N12 = 2.054(2) Å), followed by the dimeric **3a** (Mn–N12 = 2.048(1) Å), and are shortest for the cation in **2a** (Mn–N12 = 2.045(2) Å). These bond distances are comparable to those observed in related M(CO)$_3$ complexes of pyrazolyl-containing ligands such as {Mn(OH$_2$)(CO)$_3$[HN=C(CH$_3$)pz*]}(BF$_4$) (2.048(4) Å) [24] or Re(Br)(CO)$_3$(CH$_2$pz$_2$) (average 2.172(3) Å) [25]. Interestingly, the metal–nitrogen bonds of the aniline NH$_2$ group are longer in the cations of **2a/b** (Mn–N1 = 2.105(2) Å, Re–N1 = 2.226(5) Å) compared to those in the charge neutral compounds **1a/b** (Mn–N1 = 2.091(2) Å, Re–N1 = 2.219(3) Å) but are comparable to other tricarbonyl group 7 metal–aniline complexes such as those distances in [Mn(CO)$_3$(μ-*o*-SC$_6$H$_4$NH$_2$)]$_2$ (Mn–NH$_2$ average 2.094(5) Å) [26] and [Re(CO)$_3$(H$_2$N-p-tolyl)(bipy)](OSO$_2$CF$_3$) (Re–NH$_2$ 2.250(3) Å) [27]. In both **3a** and **3b**, the central planar M$_2$N$_2$ metallacycle exhibits disparate M–N bond distances (for **3a**: Mn–N1 = 2.0664(9) Å, Mn–N1* = 2.1035(9) Å; for **3b**: Re–N1 = 2.1972(15) Å, Re–N1* = 2.2270(16) Å) that, on average, are shorter than those M–NH$_2$ bonds for the corresponding complexes **1a** or **1b** (average Mn–N 2.085(2) Å; average Re–N 2.212(3) Å). The Mn–N bond distances involving the Mn$_2$N$_2$ metallacycle in **3b** are slightly shorter but similar to those in [Mn(CO)$_3$(μ-*o*-NHC$_6$H$_4$PPh$_2$)]$_2$ (Mn–N1 2.084(3) Å, Mn–N1′ 2.084(3) Å, Mn–N average 2.117(3) Å) [28]. For most of the series, the carbonyl bound *trans*- to the pyrazolyl has longer M–C bonds and shorter C–O bonds than the other two carbonyls, the exception being **3a** in which one of the carbonyls in the MnN$_2$C$_2$ equatorial plane has longer M–C bonds and shorter C–O bonds than the others. Other points of structural interest are that the mean planes of the aniline and pyrazolyl rings are not coplanar, rather the dihedral angles between planes vary without prejudice from 28° to 38° in the complexes, very similar to that seen in diphenylboryl complexes and much smaller than in the free ligand (51°) [6]. Also, for **1a/b** and **2a/b** the aniline rings are directed toward the axial carbonyl of the metal rather than the axial bromide or acetonitrile along the N12–N1 hinge axis (Fig. 1A and B gives a good view) rendering the complexes chiral with low symmetry (*C$_1$*). That is, if the complex is viewed from the perspective where two equatorial carbonyls are directed away from the viewer and the third carbonyl is oriented down (placing the ligand in the 'front' of molecule), the pyrazolyl group is oriented either toward the 'left' (such as in the top of Fig. 1) or toward the 'right' side of the molecule, giving two possible enantiomers. For each of these complexes, both enantiomers are found in the solid state

(rendering the crystals achiral) associated with one another via weak hydrogen bonding interactions as detailed in the Supporting information.

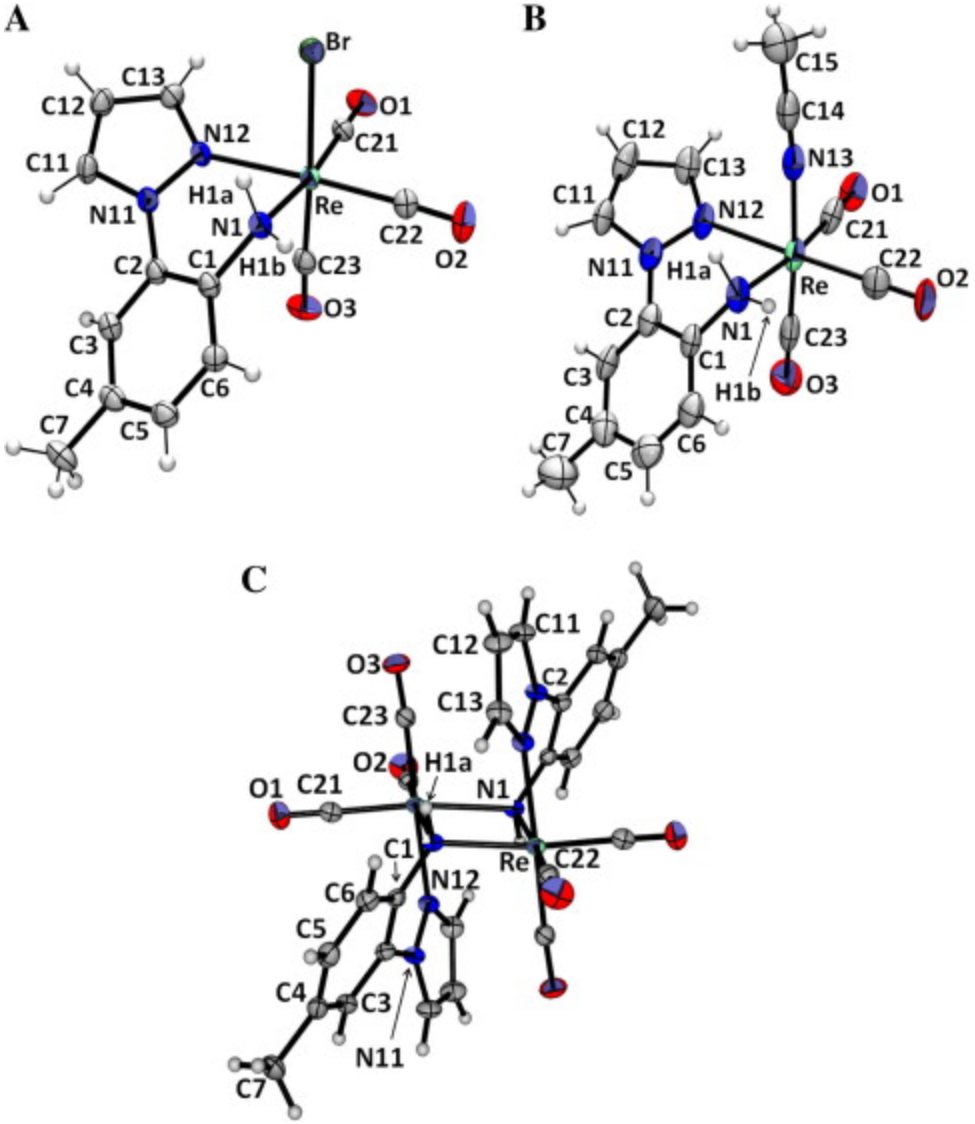

Fig. 1. ORTEP drawings (thermal ellipsoids drawn at 50% probability level) with atom labeling of structures of (A) **1b**, (B) **2b** and (C) **3b·2CH₃CN** and with anion in **2b** and solvent in **3b·2CH₃CN** removed for clarity.

Table 3. Selected bond distances and angles for $MnBr(CO)_3[H(pzAn^{Me})]$ (**1a**), $ReBr(CO)_3[H(pzAn^{Me})]$ (**1b**), $\{Mn(CH_3CN)(CO)_3[H(pzAn^{Me})]\}(PF_6)$ (**2a**), $\{Re(CH_3CN)(CO)_3[H(pzAn^{Me})]\}(PF_6)$ (**2b**), $[Mn(CO)_3(\mu\text{-}pzAn^{Me})]_2\cdot$**2CH₃CN** (**3a·2CH₃CN**), and $[Re(CO)_3(\mu\text{-}pzAn^{Me})]_2\cdot$**2CH₃CN** (**3b·2CH₃CN**) with labeling as per Fig. 1.

	1a	**1b**	**2a**	**2b**	**3a**	**3b**
Distances (Å)						
M–Br	2.5391(4)	2.6278(4)				
M–N13			2.013(2)	2.151(7)		
M–N12 (pz)	2.054(2)	2.179(3)	2.045(2)	2.180(4)	2.0478(9)	2.1696(16)

M–N1 (NH)	2.091(2)	2.219(3)	2.105(2)	2.226(5)	2.0664(9)	2.1972(15)
M_b–N1 (NH)					2.1035(9)	2.2270(16)
M–C21	1.808(2)	1.909(3)	1.807(3)	1.894(8)	1.8010(12)	1.910(2)
M–C22	1.815(2)	1.922(3)	1.836(3)	1.937(5)	1.8207(12)	1.927(2)
M–C23	1.803(2)	1.896(4)	1.802(3)	1.909(10)	1.8012(12)	1.906(2)
N1⋯N12	2.668	2.731	2.679	2.797	2.741	2.807
M⋯M					3.174	3.435
C21–O1	1.146(3)	1.152(4)	1.141(3)	1.164(9)	1.1439(15)	1.159(2)
C22–O2	1.143(3)	1.147(4)	1.134(3)	1.137(6)	1.1488(15)	1.151(3)
C23–O3	1.145(3)	1.158(4)	1.151(3)	1.160(10)	1.1470(15)	1.155(3)
Angles (°)						
N1–M–N12	80.12(8)	76.77(10)	80.38(9)	78.8(2)	83.55(4)	80.28(6)
N1–M–N1b					80.86(4)	78.13(6)
M–N1–M					99.14(4)	101.87(6)
M_{pl}(aryl)–M_{pl}(pz)	32.8	34.0	31.3	37.8	27.6	30.40

5.3. IR spectroscopy

The IR spectra of each complex in the solid state (KBr) consists of one high-energy and two lower energy C–O stretching bands, consistent with a facial tricarbonyl arrangement with local C_{3v} (MC_3N_3) or C_s (MC_3N_2Br) symmetry about the metal, where the lower energy bands are broad and partly resolved in the dimeric cases **3a** and **3b**. The C–O stretching frequencies for solutions of the complexes are, on average, shifted about 9 cm^{-1} higher in energy compared to the solid state spectra and the two lower energy bands are not resolved for the ionic species **2a/b** or the dimeric species **3a/b**. Moreover, the C–O stretching frequencies for the rhenium complexes are lower energy than those for the analogous manganese complexes owing to the more favorable energy match between the carbonyl π^* orbitals and the rhenium 5*d*-orbitals (hence greater back-bonding) vs. the manganese 3*d*-orbitals. Within a given series of metal complexes (manganese or rhenium), the carbonyl stretching frequencies follow the usual trend becoming lower in energy with the more electron-rich nature of the complex. Thus, the *ν*C–O stretches are highest in energy for cationic species (**2a** or **2b**), followed by the charge neutral bromide complexes (**1a** or **1b**), which are, in turn, higher energy than the dimeric species (**3a** or **3b**). It is noted that the solution IR spectra for the crystalline metal bromide complexes **1a** or **1b** dissolved in CH_3CN had very weak intensity bands (occurring as shoulders to the main bands) for carbonyl stretches with energies comparable to those in **2a** or **2b**. Although the relative intensities of bands were not quantified, these observations are indicative of partial dissociation of **1a/b** in CH_3CN, presumably giving $\{M(CH_3CN)(CO)_3[H(pzan^{Me})]^+\}(Br^-)$, similar to behavior reported for another related system [29]. Such weak intensity bands are absent in the CH_2Cl_2 solution IR spectra.

5.4. NMR spectroscopy

The NMR spectra for the complexes confirmed coordination of the ligand and indicated that the geometries observed in the solid state were generally retained in CH_3CN. The spectra of the manganese complexes were less informative than those of the rhenium derivatives owing to the large quadrupole moment of the ^{55}Mn nuclei that gives broad resonances and loss of $^3J_{HH}$ coupling features. Nonetheless, both integration and comparison of chemical shifts of resonances with those of the well-behaved rhenium derivatives allows for indirect interpretation of the manganese spectra. In all of the

current coordination complexes, the proton resonances for hydrogens on the pyrazolyl portion of the ligand are shifted downfield while those on the aniline are shifted upfield relative to those of the free ligand in CH_3CN. In both **1b** and **2b**, the hydrogens of the NH_2 group are resolved into a pair of broad doublets (Fig. 2) due to germinal coupling ($^2J_{HH}$ = 12 Hz) between 'axial' and 'equatorial' hydrogens of the screw-boat chelate ring conformation found in the solid state; in **1a** and **2a**, the coupling is not always observed in each of the two N–H resonances for reasons described above. The chelate ring conformations appear to be energetically locked as two NH resonances are observed even at 70 °C in CH_3CN. As also can be seen in the spectra of crystalline **1b** in CD_3CN (Fig. 2), the data consists of two sets of overlapping resonances that correspond to those anticipated for **1b** (major component, 98%) and those similar to **2b** (minor component, 2%). That is, the chemical shifts of singlet resonances for pyrazolyl hydrogens, and those for the unique aryl-H and aryl-CH_3 (not shown in Fig. 2) are identical in both the spectra of **2b** and the minor component of the spectrum of **1b** but those of the two AB aryl multiplet resonances and the two NH resonances are slightly dissimilar due to differences in counter anions (Br^- vs. PF_6^-); the Supporting information further documents the anion dependence of the chemical shifts of these latter resonances. Similar observations are made for the manganese derivatives. The minor resonances are not present when the same solid samples of **1a** or **1b** are dissolved in either acetone-d_6 or CD_2Cl_2, giving further evidence (in addition to the IR spectral data) that the minor species present in acetonitrile is likely $\{M(CD_3CN)(CO)_3[H(pzAn^{Me})]^+\}(Br^-)$ (M = Mn, Re, as appropriate). Finally, in the spectrum of **3b,** the resonance for the NH occurs at relatively high field (δ_H = 3.48 ppm) likely due to magnetic anisotropy effects experienced by this hydrogen being sandwiched between pi-clouds of both an axial carbonyl and pyrazolyl rings of adjacent metal centers.

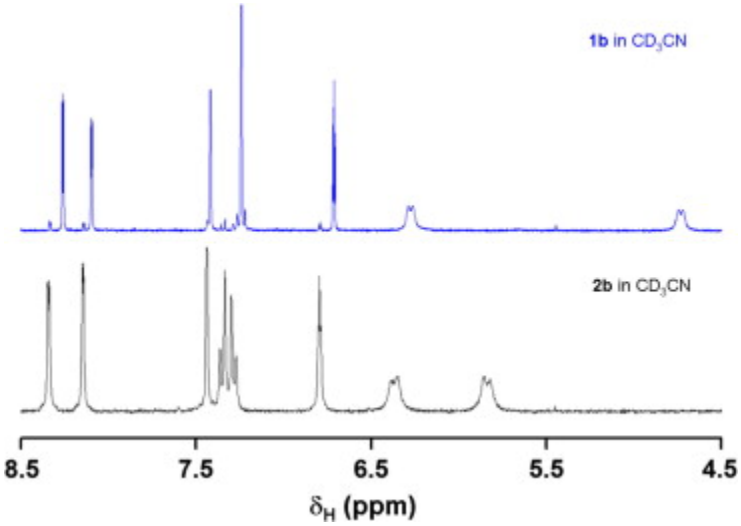

Fig. 2. A portion of the ^1H NMR spectrum of pure crystalline **1b** (top) and **2b** (bottom) dissolved in CD_3CN.

5.5. Electrochemistry

Since $M^I(CO)_3$ complexes (M = Mn, Re) [30] and the $H(pzAn^{Me})$ ligand [6] are each known electron donors, their electrochemistry was examined by cyclic voltammetry. The cyclic voltammograms for the various compounds obtained in CH_3CN are found in Fig. 3. Unfortunately, the poor solubility of the dimeric complexes **3a** and **3b** prohibited reliable electrochemical data from being obtained. The cyclic voltammogram of each metal complex **1a/b** and **2a/b** exhibits an irreversible oxidation (E_{pa} ranging

between 1.0 and 1.7 V vs. Ag/AgCl, where the cathodic wave is significantly less intense than expected, see Section 2) and an irreversible reduction (E_{pc} ranging between −1.6 and −2.1 V) at potentials more positive than that in the free ligand. The charge neutral derivatives **1a** and **1b** are more easily oxidized by about 0.4 V than the corresponding cationic derivatives **2a** and **2b**, expected from coulombic arguments. Also, the manganese(I) derivatives are more easily oxidized than the corresponding rhenium(I) complexes by about 0.3 V which parallels previous theoretical and experimental results (UV–photoelectron spectroscopy) observed for the $CpM(CO)_3$ [31] and $M(CO)_5Br$ [32] (M = Mn, Re) series of complexes, where it is noted that differences attributed to solvation and structural reorganization of isostructural Mn and Re congeners are negligible such that correlations between experimental gas phase ionization potentials and solution-phase electrochemical experiments are typically maintained [33]. Based upon experimental observations for other $H(pzAn^{Me})$ derivatives [34] as well as the frontier orbitals obtained from single point energy calculations (Supporting information) which show that the HOMO is centered on the $M(X)(CO)_3$ fragment and the LUMO is essentially a ligand π^* orbital (Fig. 4) we tentatively assign the oxidations in the group 7 metal tricarbonyl complexes as metal-centered and the reductions as ligand-centered in accord with Koopmans theorem [35].

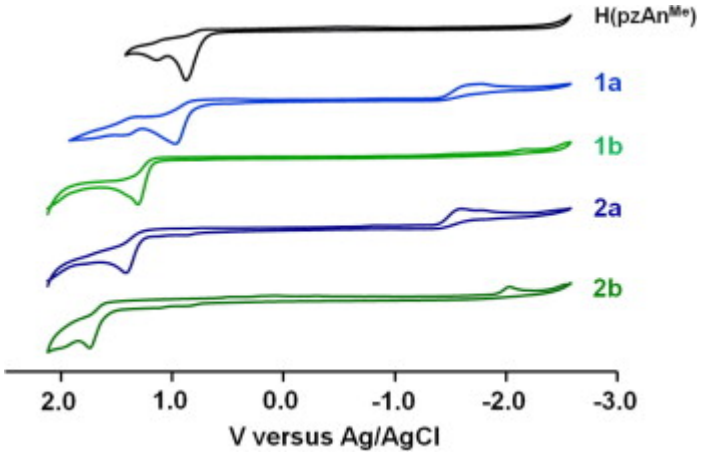

Fig. 3. Cyclic voltammograms obtained at scan rates of 50 mV/s for ligand $H(pzAn^{Me})$ (top) and metal complexes in CH_3CN with $(NBu_4)(PF_6)$ as supporting electrolyte.

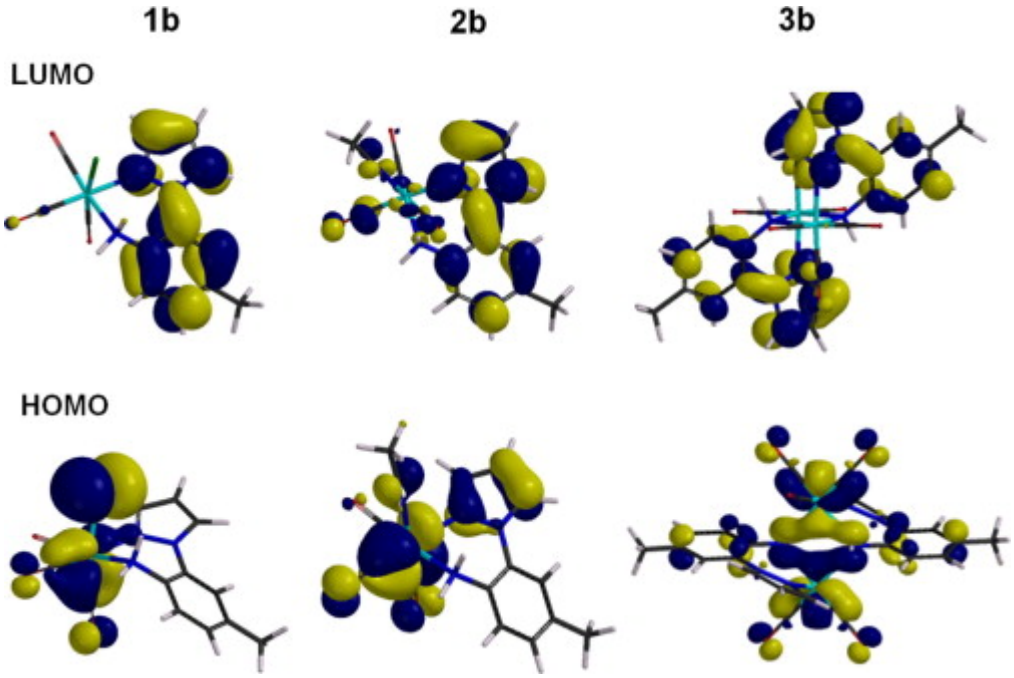

Fig. 4. Frontier orbitals [LUMO (top) and HOMO (bottom)] for rhenium complexes **1b** (left), **2b** (center) and **3b** (right) from density functional calculations (BP86/6-31G*//B3LYP/LAVCP*).

5.6. Electronic spectroscopy

The electronic absorption spectra of all six derivatives were recorded and representative spectra of **1a** and **1b** are given in Fig. 5 while complete electronic spectra are found in the Supporting information. The poor solubility of **3a** and **3b** has hindered accurate measurements of their extinction coefficients. Each of the metal complexes has a low-spin d^6 electron configuration as expected from the strong-field carbonyl ligands and as evident from their diamagnetic NMR spectrum. Thus, two *d*–*d* transitions of low intensity ($\varepsilon < 200\ M^{-1}\ cm^{-1}$) might be expected for pseudo-octahedral metal centers ($^1A_1 \rightarrow {}^1T_1$ and $^1A_1 \rightarrow {}^1T_2$) as observed in other low-spin d^6 systems [36]. Unfortunately it was not possible to observe these bands as they are likely obscured by the remainder of the absorption bands. Instead, each spectrum consists of a low-energy band $\lambda > 300$ nm of moderately low intensity ($\varepsilon \sim 2000\ M^{-1}\ cm^{-1}$) that likely corresponds to a metal-to-ligand charge transfer (*MLCT*) or a delocalized metal-ligand-to-ligand charge transfer (*MLLCT*), in analogy to the nicely detailed theoretical and experimental studies on the related $ReCl(CO)_3[HC(3,5\text{-}Me_2pz)_2]$ complex [37]. For the manganese compounds, the lowest energy band tails into the violet region of the visible spectrum giving rise to the yellow color of the compounds while the lowest energy absorption bands for the rhenium complexes are outside the visible range rendering these complexes colorless. The two medium-intensity bands ($\varepsilon \sim 10\,000$–$20\,000\ M^{-1}\ cm^{-1}$) and two, intense, high-energy bands (one occurs as a shoulder in the manganese cases) near 200 nm are likely due to π–π^* intraligand transitions based on both energy and intensity considerations. Unfortunately, in contrast to other complexes of $H(pzAn^{Me})$ and its derivatives, none of the current complexes are luminescent in solution or the solid state.

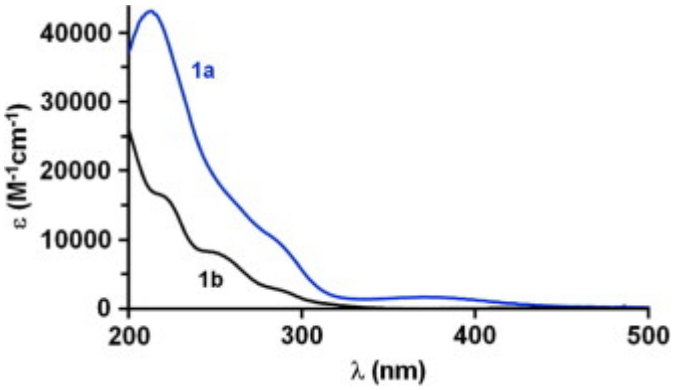

Fig. 5. Overlay of the electronic absorption spectrum of **1a** (blue line) and **1b** (black line) in CH_3CN. (For interpretation of the references to color in this figure legend, the reader is referred to the web version of this article.)

6. Concluding remarks

In this study, we began a survey of the transition metal coordination chemistry of the electron-rich, N,N-chelating H(pzAn^{Me}) ligand by exploring group 7 tricarbonyls. It was hoped that stable complexes could be obtained and that drastic changes in the electronic properties of the normally non-innocent ligand scaffold would be observed. Moreover, it was also hoped that switching behavior could be observed by cycling reactions of Brønsted acids and bases where the reaction of the complexes with Brønsted bases would restore energetic access to the lone pair on nitrogen responsible for the electron donor properties of aniline derivatives which should be otherwise inhibited when nitrogen is coordinatively-saturated. Thus, four complexes of the type $[M(X)(CO)_3[H(pzAn^{Me})]\}^{n+}$ [X = Br, *n* = 0, M = Mn (**1a**), M = Re (**1b**); X = CH_3CN, *n* = 1, M = Mn (**2a**), M = Re (**2b**)] with coordinatively-saturated toluidinyl nitrogens were prepared and characterized both in the solid state and in solution. The relative stabilities of the complexes followed the order **2b** > **2a** > **1b** > **1a** based on chemical reactivities, electrochemical, and spectroscopic properties which also follows the order expected based on both coulombic arguments and periodic trends. The reactions between any of the four complexes and $(NEt_4)(OH)$ as a Brønsted base produced the highly insoluble dimeric $[fac\text{-}M(CO)_3(\mu\text{-}pzAn^{Me})]_2$, (M = Mn (**3a**) or M = Re (**3b**)) where the amido nitrogens of the ligands bridge two six coordinate metal centers. Although none of the current complexes exhibited desirable photophysical properties (in stark contrast to chelate complexes with redox-inactive main group Lewis acids which are typically intensely fluorescent) or reversible switching behavior owing to the low solubility of **3a** and **3b**, structurally modified variants of the H(pzAn^{Me}) scaffold (using groups that prevent dimerization) can impart such behavior in their tricarbonylrhenium(I) complexes and the successful endeavors by our group in this vein will be disseminated shortly.

Acknowledgements

J.R.G. thanks Marquette University, the National Science Foundation (CHE-0848515), and the donors of the Petroleum Research Fund for support.

References

[1] (a) B.L. Oliveira, J.D.G. Correia, P.D. Raposhinho, I. Santos, A. Ferreira, C. Cordeiro, A.P. Freire. *Dalton Trans*. (2009), pp. 152-162 (b) L. Maria, S. Cunha, M. Videira, L. Gano, A. Paulo, I.C. Santos, I. Santos *Dalton Trans*. (2007), pp. 3010-3019 (c) R. Alberto. *Top. Curr. Chem*., 252 (2005), pp. 1-44 (d) J.R. Dilworth, S.J. Parrott. *Chem. Soc. Rev*., 27 (1998), pp. 43-45

[2] R.A. Kirgan, B.P. Sullivan, D.P. Rillema. *Top. Curr. Chem*., 281 (2007), pp. 45-100

[3] (a) M.E. Walther, O.S. Wenger. Dalton Trans. (2008), pp. 6311-6318. (b) GA. Vlcek, M. Busby. Coord. Chem. Rev., 250 (13&14) (2006), pp. 1755-1762

[4] (a) Z. Si, J. Li, B. Li, F. Zhao, S. Liu, W. Li. Inorg. Chem., 46 (2007), pp. 6155-6163. (b) N.J. Lundin, A.G. Blackman, K.C. Gordon, D.L. Officer. Int. Ed., 45 (2006), pp. 2582-2584

[5] (a) G.J. Meyer. Inorg. Chem., 44 (2005), pp. 6852-6864. (b) K. Kalyanasundaram, M. Gratzel. Coord. Chem. Rev., 177 (1998), pp. 347-414

[6] B.J. Liddle, R.M. Silva, T.J. Morin, F.P. Macedo, R. Shukla, S.V. Lindeman, J.R. Gardinier. J. Org. Chem., 72 (2007), pp. 5637-5646

[7] T.J. Morin, S.V. Lindeman, J.R. Gardinier. Eur. J. Inorg. Chem. (2009), pp. 104-110

[8] B.J. Liddle, S.V. Lindeman, D.L. Reger, J.R. Gardinier. Inorg. Chem., 46 (2007), pp. 8484-8486

[9] (a) A. Mukherjee, U. Subramanyam, V.G. Puranik, T.P. Mohandas, A. Sarkar. Eur. J. Inorg. Chem. (2005), pp. 1254-1263. (b) W.E. Piers, S.C. Bourke, K.D. Conroy. Angew. Chem., Int. Ed., 44 (2005), pp. 5016-5036. (c) N. Saha, A. Saha, S. Chaudhuri, T.C.W. Mak, T. Banerjee, P. Roychoudhury. Polyhedron, 11 (1992), pp. 2341-2349

[10] M.G.B. Drew, A. Mukherjee, S. De, S. Nag, D. Datta. Inorg. Chim. Acta, 360 (2007), pp. 3448-3451

[11] S.P. Schmidt, W.C. Trogler, F. Basolo. Inorg. Synth., 28 (1990), pp. 160-165

[12] I. Noviandri, K.N. Brown, D.S. Fleming, P.T. Gulyas, P.A. Lay, A.F. Masters, L. Phillips. J. Phys. Chem. B, 103 (1999), pp. 6713-6722

[13] Spartan, Wavefunction, Inc., Irvine, CA, 1997.

[14] (a) T. Takatani, J.S. Sears, D.C. Sherill. J. Phys. Chem. A, 113 (2009), pp. 9231-9236 (b) V.M. Rayon, G. Frenking. Chem. Eur. J., 8 (2002), pp. 4693-4707. View Record in Scopus (c) R.K. Szilagyi, G. Frenking. Organometallics, 16 (1997), pp. 4807-4815

[15] A.D. Becke. J. Chem. Phys., 98 (1993), pp. 5648-5652

[16] C. Lee, W. Yang, R.G. Parr. Phys. Rev. B, 37 (1988), pp. 785-789

[17] (a) P.J. Hay, W.R. Wadt. J. Chem. Phys., 82 (1985), pp. 270-283. (b) W.R. Wadt, P.J. Hay. J. Chem. Phys., 82 (1985), pp. 284-298

[18] Smart apex2 Version 2.0-2 Bruker Analytical X-ray Systems, Inc., Madison, Wisconsin, USA, 2005.

[19] Saint+ Version 7.23a and Sadabs Version 2.05, Bruker Analytical X-ray Systems, Inc., Madison, Wisconsin, USA, 2005.

[20] G.M. Sheldrick, Shelxtl Version 6.1; Bruker Analytical X-ray Systems, Inc., Madison, Wisconsin, USA, 2000.

[21] (a) H.J. Cristau, P.P. Cellier, J.F. Spindler, M. Taillefer. Eur. J. Org. Chem. (2004), pp. 695-709. (b) M. Taillefer, N. Xia, A. Ouali. Angew. Chem., Int. Ed., 46 (2007), pp. 934-936 (c) H.J. Christau, P.P. Cellier, J.F. Spindler, M. Taillefer. Chem. Eur. J., 10 (2004), pp. 5607-5622. (d) J.M. Lindley, I.M. McRobbie, O. Meth-Cohn, H. Suschitzky. J. Chem. Soc., Perkin Trans., 1 (1980), pp. 982-994

[22] J.C. Antilla, J.M. Baskin, T.E. Barder, S.L. Buchwald. J. Org. Chem., 69 (2004), pp. 5578-5587

[23] See Supporting information regarding pitfalls of another route.

[24] N. Antón, M. Arroyo, P. Gómez-Iglesias, D. Miguel, F. Villifañe. J. Organomet. Chem., 693 (2008), pp. 3074-3080
[25] D.L. Reger, J.R. Gardinier, P.J. Pellechia, M.D. Smith, K.J. Brown. Inorg. Chem., 42 (2003), pp. 7635-7643
[26] W.-F. Liaw, C.-K. Hsieh, G.-Y. Lin, G.-H. Lee. Inorg. Chem., 40 (2001), pp. 3468-3475
[27] E. Hevia, J. Perez, V. Riera, D. Miguel. Organometallics, 21 (2002), pp. 1966-1974
[28] V.D. Fester, P.J. Houghton, L. Main, B.K. Nicholson. Polyhedron, 26 (2007), pp. 430-433
[29] R.M. Silva, B.J. Liddle, S.V. Lindeman, M.D. Smith, J.R. Gardinier. Inorg. Chem., 45 (2006), pp. 6794-6802
[30] (a) J.P. Bullock, E. Carter, R. Johnson, A.T. Kennedy, S.E. Key, B.J. Kraft, D. Saxon, P. Underwood. Inorg. Chem., 47 (2008), pp. 7880-7887. (b) R. Seeber, G.A. Mazzocchin, U. Mazzi, E. Roncari, F. Refosco. Trans. Met. Chem., 9 (1984), pp. 315-318. (c) S.P. Gubin, L.I. Denisovich, N.V. Zakurin. Khim., 6 (1978), pp. 1322-1327 (d) L.I. Denisovich, N.V. Zakurin, S.P. Gubin, A.G. Ginzburg. J. Organomet. Chem., 101 (1975), pp. C43-C44
[31] R.F. Fenske, D.L. Lichtenberger. J. Am. Chem. Soc., 98 (1976), pp. 50-63
[32] M.B. Hall. J. Am. Chem. Soc., 97 (1975), pp. 2057-2065
[33] L.E. Roy, E.R. Batista, P.J. Hay. Inorg. Chem., 47 (2008), pp. 9228-9237
[34] The electrochemical behavior of aniline derivatives relies on the availability of the lone pair of electrons on the NH_2 moiety to be in conjugation with the aryl π-system rendering the aromatic molecule electron-rich. Upon binding to Lewis acids, the nitrogen becomes quartenary and its lone pair of electrons is less energetically accessible. As will be detailed elsewhere, the oxidation potentials of the protonated ligand $[H_2(pzAn^{Me})](BF_4)$ and even that of the cationic $[Me_2C(N,N\text{-}pzAnMe)](BF_4)$ (with an sp^2-hybridized amino nitrogen) occur above 2.3 V.
[35] T. Koopmans. Physica, 1 (1933), pp. 104-113
[36] (a) B.N. Figgis, M.A. Hitchman. **Ligand Field Theory and Its Applications.** Wiley-VCH, New York (2002) (b) A.B.P. Lever. **Inorganic Electronic Spectroscopy.** New York, Elsevier (1968)
[37] B. Machura, R. Kruszynski, M. Jaworska, P. Lodowski, R. Penczek, J. Kusz. Polyhedron, 27 (2008), pp. 1767-1778